

Microscopic calculation of nuclear dissipation*

S. E. Koonin[†]

Laboratory for Nuclear Science and Department of Physics, Massachusetts Institute of Technology, Cambridge, Massachusetts 02139
and Theoretical Division, Los Alamos Scientific Laboratory, University of California, Los Alamos, New Mexico 87545

J. R. Nix

Theoretical Division, Los Alamos Scientific Laboratory, University of California, Los Alamos, New Mexico 87545

(Received 2 September 1975)

By use of a time-dependent wave function of the BCS form, we compute microscopically the energy dissipated for a system with a monopole pairing force moving under the influence of a time-dependent single-particle potential. Quasiparticle generation and coupling of the two-quasiparticle modes of the system are included automatically and provide contact with the Landau-Zener formula. The single-particle potential is related to nuclear shapes generated by viscous hydrodynamical calculations of a fissioning ^{236}U nucleus. We attempt to determine the energy dissipated between the saddle point and scission point by requiring that at the scission point the energy dissipated in the microscopic calculations equal that dissipated in the macroscopic hydrodynamical calculations. This procedure leads to 34 MeV of dissipated energy, which is almost twice the value of 18 MeV obtained from macroscopic hydrodynamical calculations that reproduce experimental fission-fragment kinetic energies. The corresponding value of the nuclear viscosity coefficient determined from the microscopic calculations is 0.04 TP, compared to 0.015 ± 0.005 TP obtained from the macroscopic hydrodynamical calculations. The viscosity coefficient determined from the microscopic calculations is even larger if the dissipated energies are compared at a finite scission neck radius. As a possible resolution of this discrepancy, we propose that level splittings arising from axially asymmetric and reflection-asymmetric deformations during the descent from the saddle point to scission reduce the energy dissipation and make the nuclei only moderately viscous.

NUCLEAR REACTIONS Fission ^{236}U ; calculated microscopically energy dissipated between saddle point and scission. Monopole pairing force, time-dependent wave function of BCS form, correspondence with Landau-Zener formula, nuclear viscosity, axially asymmetric and reflection-asymmetric deformations important.

I. INTRODUCTION

The central problem in treating the dynamics of nuclear systems is similar to one that occurs in the kinetic theory of gases. This is the isolation and treatment in detail of a few physically significant *collective* variables describing the system, while at the same time handling approximately the behavior and influence of the many other *intrinsic* variables which are "swept under the rug."

Although the problem of choosing the correct set of collective variables is by no means simple or even well defined in general, once such a choice is made we are led immediately to the concept of dissipation, or the flow of energy between the collective and intrinsic modes. In large classical systems, which are characterized by such collective coordinates as density and velocity fields, this energy flow is irreversible, with organized collective motion always degrading into "heat." Such dissipation can be described in terms of a viscosity coefficient by introducing a dissipative term into the dynamical equations of motion.

In a classical hydrodynamical description of nuclear motion, dissipation is introduced convenient-

ly by means of Rayleigh's dissipation function.¹⁻¹⁰

This function, which is equal to one-half the rate at which energy is converted from collective to intrinsic degrees of freedom, is quadratic in the collective velocities. This modifies the classical Lagrange equations of motion by introducing terms that are linear in the collective velocities. Alternatively, one can attempt to solve directly the Navier-Stokes equation by use of finite-difference methods.¹¹

In a hydrodynamical approach the nuclear viscosity coefficient can be determined by comparing calculations that depend upon its value with the corresponding experimental quantities. For example, in the fission of a heavy nucleus, nuclear viscosity affects strongly the dynamical path from the fission saddle point onwards and hence the fission-fragment kinetic energy. A recent comparison^{5,6} of calculated and experimental fission-fragment kinetic energies gives for the nuclear viscosity coefficient μ the value 0.015 ± 0.005 TP, where

$$1 \text{ TP} = 1 \text{ terapoise} = 10^{12} \text{ poise} = 10^{12} \text{ dyn s/cm}^2 \\ = 6.24 \times 10^{-22} \text{ MeV s/fm}^3 = 0.948 \hbar/\text{fm}^3.$$

This is about 30% of the value that is required to critically damp the quadrupole oscillations of idealized heavy actinide nuclei. Other estimates⁸⁻¹⁰ of the nuclear viscosity coefficient based on the damping of the motion from the fission saddle point to scission, the damping of vibrational states, and the damping of giant dipole resonances also yield values of about 0.015 TP. Several other attempts have also been made to deduce information on nuclear viscosity from experimental data on fission¹²⁻²⁰ and very-heavy-ion-induced reactions,²⁰⁻⁴² as well as by other means.^{14,43}

While the description of dissipation in terms of a bulk viscosity coefficient is useful for a wide variety of classical systems, in quantal systems it is desirable to start from a more microscopic point of view. Whereas in classical systems the viscosity coefficient can be derived from microscopic kinetic-theory equations and hence related ultimately to the interparticle potential, an analogous derivation for quantal systems from the many-body Schrödinger equation has not yet been achieved. In fact, because of the relatively small number of nucleons in the nucleus, fluctuations from irreversible behavior may be quite large, allowing energy to be exchanged freely in *both* directions between collective and intrinsic coordinates.

Several studies directed toward a microscopic description of nuclear dissipation have been made already.⁴⁴⁻⁶¹ These include such varied approaches as a Fermi-fluid model,⁴⁴⁻⁴⁶ standard reaction theory,⁴⁷ and linear-response theory.^{48,49} However, the traditional microscopic interpretation of nuclear dissipation is in terms of the mechanism of slippage at level crossings.⁶²⁻⁷² In this approach the collective coordinates are taken to describe the shape of the single-particle potential, and the intrinsic coordinates to describe the configuration of the nucleons in this potential. It should be borne in mind, however, that there is considerable ambiguity in such an identification because the shape of the single-particle potential depends upon the nucleon coordinates, and collective kinetic energy must arise ultimately from changes in the intrinsic coordinates representing the flow of nuclear matter.

Under certain restrictive assumptions concerning the energies of two levels which in the absence of residual interactions would cross as the collective coordinates change, Landau^{73,74} and Zener⁷⁵ derived an expression for the probability that the system jumps from the adiabatic path to the excited state at such a level crossing. Although calculations employing the Landau-Zener formula have been used to describe dissipation during heavy-ion fusion processes,⁶⁹⁻⁷² the conditions

necessary for its validity are in fact not well satisfied in nuclear systems.

Among the first attempts at a realistic description of level slippage was an effort by Schütte and Wilets^{65,66} to relate the residual interaction of the Landau-Zener formula to the well-known pairing force that couples pairs of nucleons moving in time-reversed orbitals. By restricting themselves to a limited class of two-quasiparticle excitations of the nucleus, they were able to solve the time-dependent Schrödinger equation for motion in a simplified version of a modified spheroidal harmonic-oscillator potential and thereby demonstrate the dissipation of energy from collective modes into intrinsic modes.

In this paper we first reformulate and extend the idea of Schütte and Wilets and second treat a realistic situation in an attempt to determine the nuclear viscosity coefficient. To these ends we show in Sec. II how dissipation in a system with a pairing-force residual interaction may be treated in general, allowing in a simple way the simultaneous inclusion of multiquasiparticle states. Expressions are derived for the time evolution of the one-body density matrix and pairing-field matrix, which are then related to the usual time-dependent BCS pairing amplitudes u and v .⁷⁶ Our expressions for the rate of energy dissipation show that in general the dissipation is not irreversible. The latter part of this section discusses level slippage as embodied in this formalism and explores the connection to the Landau-Zener formula. The determination of the nuclear viscosity coefficient proceeds in Sec. III, where we treat the descent of ²³⁶U from its macroscopic saddle point to scission. Although we determine a value of the nuclear viscosity coefficient which is consistent with the energy dissipated microscopically, there are certain inadequacies in the irreversible macroscopic parametrization, as well as ambiguities in the microscopic calculation. In Sec. IV we present our conclusions and indicate possible extensions of the calculations.

II. TIME-DEPENDENT PAIRING EQUATIONS

The simplest microscopic description of nuclear dynamics during fission is achieved by imagining that the fissioning system provides a time-dependent single-particle potential $U(t)$ in which the nucleons move independently.⁶² Such a description is within the spirit of (indeed, is the essence of) the more rigorous time-dependent Hartree-Fock (TDHF) approximation,⁷⁶ which defines U self-consistently in terms of the instantaneous positions of the nucleons and the fundamental two-nucleon interaction by constraining the many-body wave function to be a Slater determinant.

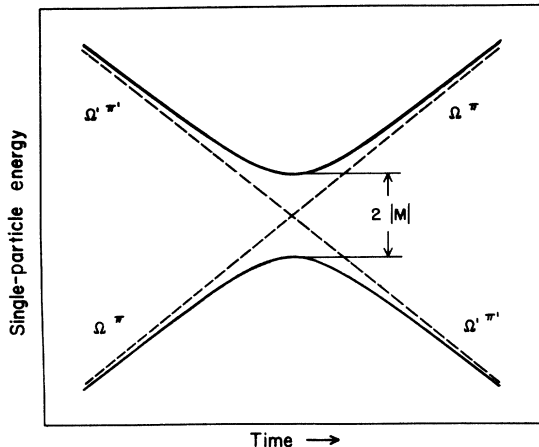


FIG. 1. Typical level crossing for a potential $U(t)$ that has axial and reflection symmetry. Levels with different values of the projection Ω of the total angular momentum on the symmetry axis and parity π cross as dashed lines. The solid lines show the time-dependent eigenstates of the full Hamiltonian, which mixes the unperturbed states with strength $|M|$. The residual interaction permits a pair of particles initially in Ω, π to shift to Ω', π' after the crossing.

The early work of Landau^{73,74} and of Zener⁷⁵ provides an important result concerning the behavior of the system at level crossings, although for a highly simplified case. If, as illustrated in Fig. 1, the energies of the crossing levels are linear functions of time and if the residual interaction is constant in time, the two-level time-dependent Schrödinger equation may be solved approximately. This yields the result

$$P_{\text{jump}} = \exp\left(-\frac{2\pi|M|^2}{d|\epsilon - \epsilon'/dt|}\right), \quad (1)$$

where P_{jump} is the probability that as the time $t \rightarrow \infty$ the system has jumped from the lower level to the upper level, M is the matrix element of the residual interaction that couples the levels, and $d|\epsilon - \epsilon'|/dt$ is the constant relative slope of the configuration energies with respect to time. Here, as throughout this paper, we use units in which $\hbar = 1$. If $|M|$ is large or if the relative slope is small (corresponding to U changing slowly with time), the adiabatic path is favored.

In nuclear systems, the validity of Eq. (1) is *a priori* highly questionable. Realistic levels do not cross as infinite straight lines. In addition, a particular level usually is crossed successively by many different levels, so that the problem is intrinsically a many-body one. The problem therefore cannot be described in terms of occupation probabilities alone, as is suggested naively by Eq. (1), but requires instead that we consider the in-

terference of amplitudes.

The time-dependent many-body problem, with a more realistic treatment of the residual interaction, may be solved in principle within the BCS formalism by use of the time-dependent Hartree-Fock-Bogoliubov (TDHFB) approximation.⁷⁶ The many-body wave function is constrained to be of the BCS form at all times, and as such is not a state of definite particle number. A TDHFB calculation is fully self-consistent in the same sense as TDHF, and level slippage is treated automatically due to the simultaneous presence of many different Slater determinants in the wave function. However, even with a simple effective nucleon-nucleon interaction such as the Skyrme interaction,^{77,78} such calculations present formidable numerical difficulties. Because of this, it is reasonable to seek a simple way in which the problems of TDHFB calculations may be bypassed, so as to obtain a qualitative estimate of the effects of the residual interaction as would be embodied in a full calculation.

The treatment of the residual interaction may be simplified considerably through the use of a monopole pairing force.^{79,80} Although this force does not reproduce more realistic forces in detail,⁸¹ it may be adjusted so as to reproduce average effects correctly, while at the same time offering much in the way of numerical simplicity.

A. Derivation

We assume for the moment that the time-dependent single-particle potential $U(t)$, as derived for example from the TDHF approximation, is known, as are the single-particle eigenfunctions and eigenvalues of the corresponding one-body Hamiltonian. We may then take the time-dependent many-body Hamiltonian to be of the form

$$H(t) = \sum_{i>0} \epsilon_i(t)(a_i^\dagger a_i + a_{-i}^\dagger a_{-i}) - G(t) \sum_{i,j>0} a_i^\dagger a_{-i}^\dagger a_{-j} a_j, \quad (2)$$

which corresponds to particles with a pairing force moving in a time-dependent single-particle potential. Here a_i^\dagger and a_i denote operators for creating and destroying, respectively, a particle in state i , $\epsilon_i(t)$ is the time-dependent eigenvalue associated with the state i , and $-i$ denotes the time-reversed orbital conjugate to, and degenerate with, i . The single-particle sum in Eq. (2) runs over only one partner of each time-reversed pair; the restricted sum in the two-body force, denoted by a prime, allows the pairing force to operate over only a finite number of active levels near the sharp Fermi surface. The pairing force acts separately between neutrons and protons; it is understood throughout the paper that all our expressions include analo-

gous terms for neutrons and protons. We henceforth consider only systems with an even number of particles (even-even nuclei).

With the Hamiltonian (2), the BCS wave function for the system is described conveniently in terms of the Hermitian one-body density matrix and symmetric pairing-field matrix defined in terms of the instantaneous eigenstates of U , namely

$$\rho_{ij}(t) \equiv \langle a_i^\dagger a_j \rangle \quad (3a)$$

and

$$\kappa_{ij}(t) \equiv \langle a_i a_{-j} \rangle. \quad (3b)$$

The brackets $\langle \rangle$ denote expectation value within the system's full time-dependent wave function.

Dynamical equations describing the time evolution of these quantities within the TDHFB formalism are derived from Heisenberg's form of the equations of motion. As discussed in detail in Appendix A, we obtain, in matrix notation,

$$\begin{aligned} i\dot{\rho} = & [\rho, \epsilon] - G\rho\rho^* - G\kappa^\dagger \text{Tr}\kappa + G\rho^*\rho + G\kappa \text{Tr}\kappa^* \\ & + i[\rho, D] \end{aligned} \quad (4a)$$

and

$$\begin{aligned} i\dot{\kappa} = & \{\kappa, \epsilon\} - G\kappa\rho^* + G\rho^* \text{Tr}\kappa + G\rho \text{Tr}\kappa - G \text{Tr}\kappa \\ & - G\rho\kappa + i[\kappa, D]. \end{aligned} \quad (4b)$$

We denote total differentiation with respect to time by a dot, complex conjugation by an asterisk, an adjoint matrix by a dagger, a commutator by square brackets, and an anticommutator by curly braces. Furthermore, ϵ is the time-dependent diagonal matrix of single-particle energies $\epsilon_i(t)$, and D is the antisymmetric time-derivative matrix for the wave functions, defined for $i \neq j$ as

$$D_{ij} = \left\langle i \left| \frac{\partial}{\partial t} \right| j \right\rangle = \left\langle i \left| \frac{\partial U}{\partial t} \right| j \right\rangle / (\epsilon_j - \epsilon_i) = -D_{ji}; \quad (5)$$

the diagonal elements of D are zero. In addition, Eqs. (4) are written with the summation convention that all matrix operations such as trace or product occurring in terms proportional to G are restricted to active levels with positive subscript in intermediate sums.

Equations (4) constitute an approximation to the TDHFB equations with a monopole pairing force which is valid when the pairing is weak and does not redistribute the nucleons so as to change significantly the potential $U(t)$. The full solution of Eqs. (4) would tell us how the entire system responds to the changing single-particle potential. The difference at a given point between the total energy and the corresponding ground-state energy for that shape would contain both energy of collective motion and internal excitation energy. The

crux of the problem is to separate the collective energy associated with the coherent movement of the nucleons from the internal excitations associated with the random motion of the nucleons. No fully satisfactory method for making this separation has been developed, and the approximate procedure that we employ is only a first step in this direction.

Our separation procedure is motivated by the observation that under certain conditions the primary contribution to the collective kinetic energy arises from terms involving the derivative matrix D defined by Eq. (5). This is true, for example, for slow collective velocities and high excitation energies, where the excitations are mainly of single-particle character. Then the matrix elements with respect to the many-body states of the system that appear in the cranking formula⁸² for the inertia tensor are approximately proportional to linear combinations of the matrix elements D_{ij} with respect to the single-particle states. Therefore, for this case, use of the approximation $D_{ij} = 0$ would give approximately zero for the collective inertia tensor when calculated from the cranking formula. We therefore attempt to eliminate the major part of the collective kinetic energy by setting the derivative matrix D equal to zero. The remaining terms in the equations of motion (4) then should describe the effect of the residual interaction on the dissipation. A similar approximation has been used also by Glas and Mosel.^{69,72}

When the system is near the ground state at slow collective velocities, our approximation $D_{ij} = 0$ is not sufficient to eliminate the major part of the collective kinetic energy. In this case the many-body states are combinations of quasiparticle states, and the resulting matrix elements that appear in the cranking formula contain large contributions in addition to the terms that are proportional to D_{ij} . Therefore, while the system is near the ground state a large fraction of the energy that we later identify as dissipated energy is in fact collective kinetic energy. But in practice this deficiency is not serious because the total amount of energy involved is relatively small when the system is still near its ground state.

At high collective velocities the cranking expression for the inertia is no longer valid and consequently it is not possible to say *a priori* to what extent the approximation $D_{ij} = 0$ should eliminate the collective kinetic energy. However, as we show later in connection with Fig. 9, in the rapid descent of a ^{236}U nucleus from its saddle point to the point at which the dissipated energy is a maximum, the contribution to the "dissipated" energy from collective kinetic energy is less than 5.1 MeV or 8%. Also, it may be seen later from Eqs. (8)

that in the absence of pairing the single particles remain in the same state irrespective of the collective velocity. Therefore, in this limiting case the dissipated energy should contain only small contributions from collective effects. Nevertheless, the separation that we have employed demands more careful study.

In a system without residual interaction, the neglect of D would permit particles to change their energy eigenvalue only and never their orbital (although of course these orbitals are changing with time). The presence of the pairing force is then the only mechanism for level slippage, and Eqs. (4) become equivalent to the assumption of a time-dependent BCS wave function of the form

$$|\Psi(t)\rangle = \prod_{j>0} [u_j(t) + v_j(t)a_j^\dagger a_{-j}^\dagger] |0\rangle, \quad (6)$$

where $|\Psi(t)\rangle$ is the many-body wave function for the system, $|0\rangle$ is the particle vacuum, and v_j and u_j are the complex BCS occupation and vacancy amplitudes, respectively; these satisfy

$$|u_j(t)|^2 + |v_j(t)|^2 = 1.$$

The one-body density and pairing fields then become diagonal in the time-dependent representation of single-particle states and are given by

$$\rho_j \equiv \rho_{jj} = |v_j(t)|^2 \quad (7a)$$

and

$$\kappa_j \equiv \kappa_{jj} = u_j^*(t)v_j(t). \quad (7b)$$

Thus ρ is real, while

$$\rho_j^2 + |\kappa_j|^2 = \rho_j.$$

Equations (4) then become

$$\dot{\rho}_j = 2G \text{Im}(\kappa_j \text{Tr} \kappa^*) \quad (8a)$$

and

$$\dot{\kappa}_j = -2i[\epsilon_j \kappa_j - G \kappa_j \rho_j + G(\rho_j - \frac{1}{2}) \text{Tr} \kappa], \quad (8b)$$

where

$$\text{Tr} \kappa = \sum_{k>0} \kappa_k.$$

For inactive orbitals $\kappa_j = 0$, whereas $\rho_j = 1$ for those below the active region of levels and 0 for those above.

Equations (8) involve only the single-particle energies $\epsilon_j(t)$, which avoids the necessity of dealing with the details of the eigenstates of U . They conserve the average number of particles in the system, $2 \text{Tr} \rho$, as may be verified by taking the trace of Eq. (8a). The total energy of the system within the TDHFB approximation is expressed simply in terms of ρ and κ as

$$E(t) \equiv \langle H \rangle = 2 \text{Tr}(\epsilon \rho) - G |\text{Tr} \kappa|^2 - G \text{Tr}(\rho^2). \quad (9)$$

By use of Eqs. (8), $E(t)$ is found to evolve in time according to

$$\dot{E}(t) = 2 \text{Tr}(\dot{\epsilon} \rho) - \dot{G} [|\text{Tr} \kappa|^2 + \text{Tr}(\rho^2)]. \quad (10)$$

Thus, in a static system, for which $\dot{\epsilon} = 0$ and $\dot{G} = 0$, the total energy is conserved, even though the individual elements of ρ and κ may still be varying with time.

B. Limiting cases

Several properties of Eqs. (8) are illuminated by studying them for the BCS ground state of a static system. The real ground-state amplitudes \bar{u}_j and \bar{v}_j then satisfy the well-known gap equations⁸⁰

$$\bar{u}_j^2 + \bar{v}_j^2 = 1 \quad (11)$$

and

$$2(\epsilon_j - \lambda) \bar{u}_j \bar{v}_j = (\bar{u}_j^2 - \bar{v}_j^2)(\Delta - G \bar{u}_j \bar{v}_j). \quad (12)$$

The pairing gap Δ is given by

$$\Delta = G \sum_{k>0}' \bar{u}_k \bar{v}_k, \quad (13)$$

and the chemical potential λ is adjusted so that

$$\sum_{k>0}' \bar{v}_k^2 = N, \quad (14)$$

where N is the number of pairs of particles involved in the pairing interaction. The ground-state energy is given by

$$E_0 = 2 \sum_{j>0}' \epsilon_j \bar{v}_j^2 - \Delta^2/G - G \sum_{j>0}' \bar{v}_j^4, \quad (15)$$

which is constant by virtue of Eq. (10).

If at time $t=0$ we insert $\rho_j = \bar{v}_j^2$ and $\kappa_j = \bar{u}_j \bar{v}_j$ as initial conditions into Eqs. (8), we find that at later times

$$\rho_j(t) = \rho_j(0) = \bar{v}_j^2$$

and

$$\begin{aligned} \kappa_j(t) &= \kappa_j(0) \exp[-i(2\lambda - G)t] \\ &= \bar{u}_j \bar{v}_j \exp[-i(2\lambda - G)t]. \end{aligned}$$

Thus each κ_j contains the same oscillating phase factor. It is precisely this delicate phase coherency which keeps ρ_j constant, as is seen by the form of Eq. (8a). In a dynamic system, it is the destruction of this coherency among the various κ_j that is responsible for the shifting of occupation probabilities as the system evolves in time.

Another interesting property of Eqs. (8) illustrates the many-body nature of the level-slippage mechanism embodied in them. If, in a dynamic system, G is small enough so that at time $t=0$ there exists no BCS solution to the static problem, all ρ_j remain constant in time (1 if the level j was

initially below the sharp Fermi surface and 0 if it was initially above), and all κ_j remain 0. Because there is *no* slippage at level crossings, the system is highly nonadiabatic, despite the existence of the pairing force. This results from a breakdown of the BCS approximation for very small values of G .

C. Definition of dissipated energy

From the above discussions, a reasonable definition of the energy dissipated after time t is

$$E^*(t) = E(t) - E_0(t), \quad (16)$$

where $E_0(t)$ is obtained from Eq. (15) by solving Eqs. (11)–(14) with the instantaneous values of $\epsilon_i(t)$ and $G(t)$. If no superconducting solution exists, the normal solution is to be used. In addition to the approximation that we have used to eliminate the collective kinetic energy, there is a difficulty associated with the interpretation of the energy that we identify as dissipated energy. Of course, our calculation is microscopically reversible in the sense that if *all* coordinates are time-reversed the system retraces its path. However, true dissipation must be macroscopically irreversible. By this we mean that the energy must remain as internal excitation energy if at some point only the macroscopic coordinates are time-reversed. This could be investigated in a microscopic calculation by a randomization of the intrinsic coordinates upon time reversal. Although clearly important, a discussion of the macroscopic irreversibility of our results is beyond the scope of the present investigation. We assume simply that the major fraction of our dissipated energy is macroscopically irreversible. In summary, the use of Eq. (16) to obtain the dissipated energy is a major uncertainty in our work.

D. Relationship to the Landau-Zener formula

The connection between the above time-dependent pairing equations and the usual Landau-Zener picture of level crossings is not at all obvious. In order to explore this connection, we describe first the coupling of the superconducting state to the excited states of the system, and then derive the effective Landau-Zener matrix element that couples crossing quasiparticle (QP) levels.

A convenient representation of the pairing Hamiltonian is in terms of the quasiparticle excitations of the system, in which $H(t)$ takes the form^{79,80}

$$H(t) = E_0(t) + \sum_{i>0} e_i(t) (\alpha_i^\dagger \alpha_i + \alpha_{-i}^\dagger \alpha_{-i}) + H_{\text{res}}(t). \quad (17)$$

The instantaneous QP energies e_i are given by

$$e_i = [(\epsilon_i - \lambda - G\bar{v}_i^2)^2 + \Delta^2]^{1/2}, \quad (18)$$

where λ , Δ , and \bar{v}_i^2 are determined by the instantaneous solution of Eqs. (11)–(14). The QP operators are given by

$$\alpha_i = \bar{u}_i a_i - \bar{v}_i a_{-i}^\dagger$$

and

$$\alpha_{-i} = \bar{u}_i a_{-i} + \bar{v}_i a_i^\dagger.$$

The instantaneous BCS ground state $|O(t)\rangle$ is the QP vacuum. In the usual treatment of the pairing problem the residual 2QP interaction $H_{\text{res}}(t)$ is neglected, so that the 2QP excitations $\alpha_i^\dagger \alpha_{-i}^\dagger |O(t)\rangle$ are the time-dependent normal modes of the system.

A typical spectrum of the system is shown as a function of time in Fig. 2. From Eq. (18), we see that the excited states are separated by $\approx 2\Delta(t)$ from the ground state. How is it, then, that the ground state, which is never crossed by another level, can be coupled to the excited QP states? The answer lies in the time dependence of $H(t)$ and hence $|O(t)\rangle$. Indeed, $|O(t)\rangle$ has a time dependence given by

$$\begin{aligned} \frac{d}{dt} |O(t)\rangle &= \sum_{j>0}' \left[\frac{d}{dt} (\bar{u}_j + \bar{v}_j a_j^\dagger a_{-j}^\dagger) \prod_{k \neq j} (\bar{u}_k + \bar{v}_k a_k^\dagger a_{-k}^\dagger) \right] |0\rangle \\ &= \sum_{j>0}' \frac{d\bar{v}_j/dt}{\bar{u}_j} \alpha_j^\dagger \alpha_{-j}^\dagger |O(t)\rangle. \end{aligned}$$

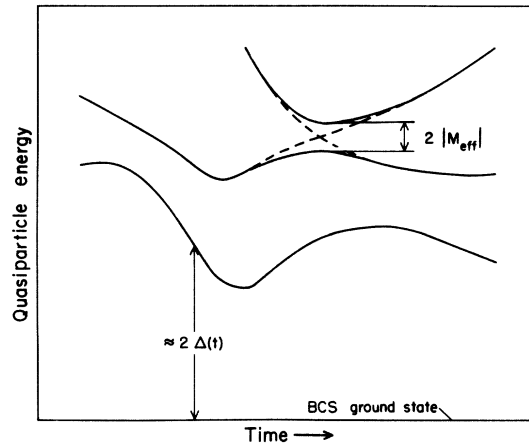


FIG. 2. Typical spectrum of a system with the pairing interaction as a function of time. The excited states are separated from the ground state by $\approx 2\Delta$. In the absence of the residual quasiparticle interaction, quasiparticle levels cross when the corresponding single-particle levels cross, as indicated by the dashed lines. However, as shown by the solid lines, the residual quasiparticle interaction splits the states, such as in Fig. 1. Note, however, that whereas Fig. 1 refers to single-particle levels, this figure refers to excitations involving the whole system.

Thus, quasiparticles are generated in orbitals j at rates proportional to $d\bar{v}_j/dt$ and hence to the velocity of the system. Note that \bar{v}_j changes not only in response to variations in ϵ_j but also because of changes in the gross parameters Δ and λ . Quasiparticles are excited most easily near the Fermi surface, where the rapid variation of \bar{v}_j with single-particle energy causes $d\bar{v}_j/dt$ to be large even for relatively small temporal variations in Δ or λ .

Contact with the Landau-Zener formula is now achieved by examining the coupling of normal modes embodied in Eqs. (8). Such coupling may be investigated by computing the random-phase-approximation (RPA) modes of the system with a pairing interaction, which are obtained by linearizing Eqs. (8) about the BCS ground state.^{76,79,80} This is done in Appendix B, where we find that the excited-state energies are given by

$$\omega_i = 2\sqrt{\lambda_i},$$

where λ_i is an eigenvalue of the matrix T defined by

$$T = \eta^2 + \Delta^2 - \Delta G \bar{u} \bar{v} + G n Q \eta + G [n \eta + G(N - \frac{1}{2} N_p) n - \Delta \bar{u} \bar{v} + G \bar{u}^2 \bar{v}^2] Q. \quad (19)$$

The matrix T is of dimension N_p by N_p , where N_p is the number of pairs of time-reversed orbitals participating in the pairing interaction. The matrices \bar{u} , \bar{v} , n , and η are diagonal, with diagonal elements given by

$$\bar{u}_{ii} = \bar{u}_i, \quad (20a)$$

$$\bar{v}_{ii} = \bar{v}_i, \quad (20b)$$

$$n_{ii} = \bar{v}_i^2 - \frac{1}{2}, \quad (20c)$$

and

$$\eta_{ii} = \epsilon_i - \lambda - G n_{ii}. \quad (20d)$$

A unit matrix is implicit in the Δ^2 term. The quantity N is the number of pairs of particles included in the pairing calculation, and Q is a matrix whose elements are all 1.

For widely separated QP energies, the noninteracting 2QP states are a good approximation to the true normal modes of the system.⁸³ In this case, the diagonal elements of T give the eigenvalues λ_i , so that the normal-mode frequencies are, neglecting terms of $\mathcal{O}(G/\Delta)$,

$$\omega_i = 2[(\epsilon_i - \lambda)^2 + \Delta^2]^{1/2},$$

which is, to within terms of the neglected order, the standard 2QP result.

However, when the single-particle spectrum contains a level crossing, so that two QP energies are very close or degenerate, a more careful treatment of the coupling terms in T is necessary. We

therefore consider a case in which two single-particle levels are degenerate, with common values of ϵ_i , \bar{u}_i , and \bar{v}_i . In this degenerate subspace T becomes

$$T = \begin{bmatrix} A & B \\ B & A \end{bmatrix},$$

where

$$A = (\epsilon_i - \lambda)^2 + \Delta^2 - 2\Delta G \bar{u}_i \bar{v}_i + G^2 [2\bar{u}_i^2 \bar{v}_i^2 - \frac{1}{4} + (N - \frac{1}{2} N_p) n_i]$$

and

$$B = 2G n_i \eta_i + G^2 (N - \frac{1}{2} N_p) m_i - \Delta G \bar{u}_i \bar{v}_i + G^2 \bar{u}_i^2 \bar{v}_i^2.$$

The corresponding 2QP levels are therefore split, with frequencies

$$\omega_{\pm} = 2(A \pm |B|)^{1/2} \approx 2\sqrt{A} \pm |B|/\sqrt{A} \equiv 2\sqrt{A} \pm |M_{\text{eff}}|,$$

where we have assumed that $|B| \ll A$. The magnitude of the effective coupling matrix element M_{eff} gives one-half the splitting.

To estimate the magnitude of the effective matrix element we take $N = \frac{1}{2} N_p$ for simplicity (this equality holds exactly for the realistic case considered in the following section). Then, by dropping terms of order G/Δ , we find that for levels crossing near the Fermi surface

$$\epsilon_i \approx \lambda, \quad \bar{v}_i \approx 1/\sqrt{2}, \quad A \approx \Delta^2, \quad \text{and} \quad |B| \approx \frac{1}{2} \Delta G,$$

which leads to

$$|M_{\text{eff}}| \approx \frac{1}{2} G.$$

For levels crossing far from the Fermi surface, we find instead that

$$A \approx (\epsilon_i - \lambda)^2 \quad \text{and} \quad B \approx G(\epsilon_i - \lambda),$$

which leads to

$$|M_{\text{eff}}| \approx G.$$

The effective Landau-Zener coupling is therefore of the order of the pairing strength G .

In summary, we have illustrated that Eqs. (8) contain two distinct processes: (1) the creation of QP pairs due to the changing ground-state BCS amplitudes and (2) the coupling of the 2QP states among themselves, which causes level slippage at crossings. In the latter process the effective Landau-Zener matrix element depends upon the energy of the crossing levels. It should be stressed, however, that while these processes describe the dynamics of the system near its ground state, the effects of nonlinear coupling to more complicated

states are also present in Eqs. (8) and are important for nonadiabatic systems.

III. DETERMINATION OF THE NUCLEAR VISCOSITY

We now proceed to a more realistic situation in an effort to determine the nuclear viscosity coefficient. No completely satisfactory method exists for incorporating the microscopic treatment of Sec. II into a macroscopic hydrodynamical model in order to obtain dynamical equations that describe simultaneously both types of degrees of freedom. Our approach is to study microscopically the energy dissipated as a function of the rate of descent of a fissioning nucleus from its saddle point to scission point. The rate of descent is obtained in turn from macroscopic hydrodynamical calculations that are performed as a function of the nuclear viscosity coefficient. We then attempt to determine the viscosity coefficient by demanding self-consistency between the energy dissipated in the microscopic calculations and that dissipated in the macroscopic calculations.

A. Description of the calculation

We consider the fission of a ^{236}U nucleus that initially is set in motion from its macroscopic saddle point with 1 MeV of kinetic energy in the fission mode. The reflection-symmetric and axially symmetric system is studied during its descent to the scission configuration. The total calculation is divided into five steps: (1) We first perform a classical macroscopic hydrodynamical calculation with a given value of the nuclear viscosity coefficient in order to determine a sequence of shapes for the fissioning system. (2) From the shapes as a function of time we determine the instantaneous single-particle potential $U(t)$ and the single-particle eigenvalues $\epsilon_i(t)$. (3) We obtain the pairing strength $G(t)$ that is required to yield a constant average pairing gap $\bar{\Delta}$. (4) We integrate the time-dependent pairing Eqs. (8) for initial conditions at the saddle point corresponding to the BCS ground state. Then from Eq. (16) we find the energy $E^*(t)$ dissipated microscopically along the fission path. (5) We compare $E^*(t)$ with the energy $E_d(t)$ dissipated in the macroscopic hydrodynamical calculation. By varying the viscosity coefficient in the macroscopic hydrodynamical calculations until the two energies are equal we hope to determine the viscosity coefficient. We now consider each of these steps in greater detail.

1. Shape sequence

Classical macroscopic hydrodynamical calculations have been performed for ^{236}U as a function of

the nuclear viscosity coefficient.^{5,6} In these calculations the nuclear shape is parametrized in terms of smoothly joined portions of three quadratic surfaces of revolution.⁸⁴ The nuclear macroscopic energy is calculated in terms of a double volume integral of a Yukawa function, which includes the surface energy of the liquid-drop model but also takes into account the lowering in energy due to the finite range of the nuclear force.^{4-6,85,86} The kinetic energy of collective nuclear motion is calculated for incompressible, nearly irrotational hydrodynamical flow. Nuclear viscosity is included by means of Rayleigh's dissipation function. The resulting modified Lagrange equations of motion are solved numerically as functions of time to yield a sequence of nuclear shapes, as well as the energy $E_d(t)$ dissipated macroscopically. For initial conditions corresponding to starting at the saddle point with 1 MeV of kinetic energy in the fission direction, Fig. 3 shows how the nuclear shapes evolve in time for various values of the nuclear viscosity coefficient μ . A comparison of calculated and experimental fission-fragment kinetic energies for nuclei throughout the Periodic Table yields for μ the value 0.015 ± 0.005 TP.

2. Single-particle energies

We generate a time-dependent diffuse-surface single-particle potential by folding a Yukawa function over the uniform sharp-surface shapes^{87,88} for the $\mu = 0.02$ TP hydrodynamical path. The total potential $U(t)$ contains also a spin-orbit term and, for protons, a Coulomb potential. With this potential the Schrödinger equation is solved by expanding the wave functions in deformed harmonic-oscillator basis functions.^{2,87} This yields the single-particle energies $\epsilon_i(t)$ as functions of time along the $\mu = 0.02$ TP hydrodynamical path. Figures 4 and 5 show the resulting level diagrams for neutrons and protons, respectively. Note in these figures the rapid variations in the single-particle levels $\epsilon_i(t)$ for a neck radius $\geq 0.5R_0$, followed by relatively smooth variations down to the scission configuration. Hence, if other conditions are equal, it is easier to excite the system near the saddle point than near the scission point.

In order to avoid the large amount of computation which would be required to construct similar diagrams along shape sequences generated by different values of the nuclear viscosity coefficient, we perform the following scaling process. For each hydrodynamical path, the neck radius of the nuclear shape is computed as a function of time, as shown in Fig. 6. The single-particle energies are then assumed to be the same functions of the neck radius along all paths. This maps all the dy-

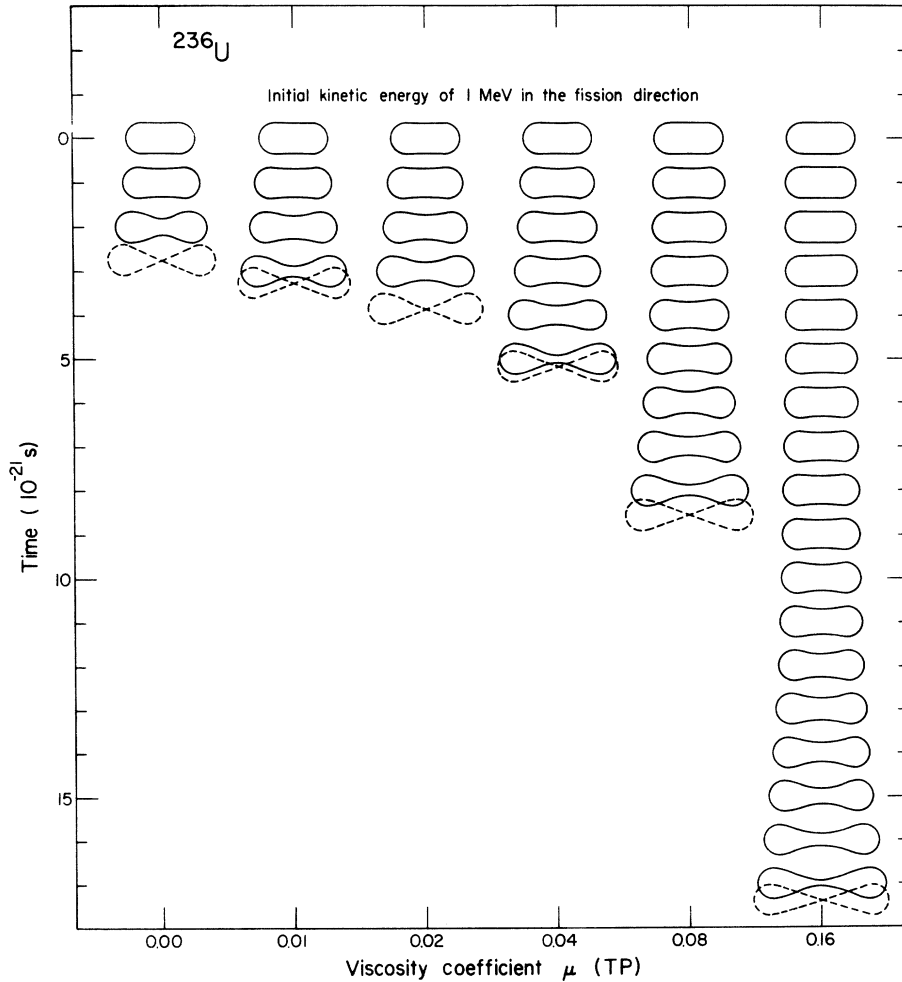


FIG. 3. Shapes of a ^{236}U nucleus from the saddle point to scission, calculated in a macroscopic hydrodynamical model for various values of the viscosity coefficient μ . The initial conditions in each case correspond to starting from the saddle point with 1 MeV of kinetic energy in the fission direction. The scission shapes are shown dashed.

namical paths onto the $\mu = 0.02$ TP path, although of course at different times. The actual levels are calculated for a sequence of shapes along the $\mu = 0.02$ TP path corresponding to steps of $0.1R_0$ in the distance r between the centers of mass of the two halves of the system, where the radius R_0 of the spherical nucleus is given by $R_0 = (1.16 \text{ fm})A^{1/3} = 7.17 \text{ fm}$. The values of ϵ_i needed at intermediate points are found by cubic interpolation of the neighboring known values.

3. Pairing strength

The magnitude and variation of the pairing strength $G(t)$ is somewhat uncertain. Although properties of the ground state and low-lying excited states permit G to be determined for ground-state shapes, little is known about the pairing interaction for the highly deformed shapes considered

here. We determine G by requiring that the average pairing gap $\bar{\Delta}$ for a uniform distribution of levels be fixed for both neutrons and protons at its phenomenologically determined value of^{87, 89}

$$\bar{\Delta} = C/\sqrt{A},$$

where

$$C = 12 \pm 1 \text{ MeV}.$$

The average pairing gap $\bar{\Delta}$ is computed for a uniform distribution of active levels whose density of pairs $\bar{\rho}(t)$ equals that obtained by means of a Strutinsky smoothing process at the smooth Fermi surface. The corresponding value of $G(t)$ is then obtained from^{2, 87}

$$\frac{1}{G(t)} = \bar{\rho}(t) \ln \left(\left\{ \left[\frac{N_p}{2\bar{\rho}(t)\bar{\Delta}} \right]^2 + 1 \right\}^{1/2} + \frac{N_p}{2\bar{\rho}(t)\bar{\Delta}} \right),$$

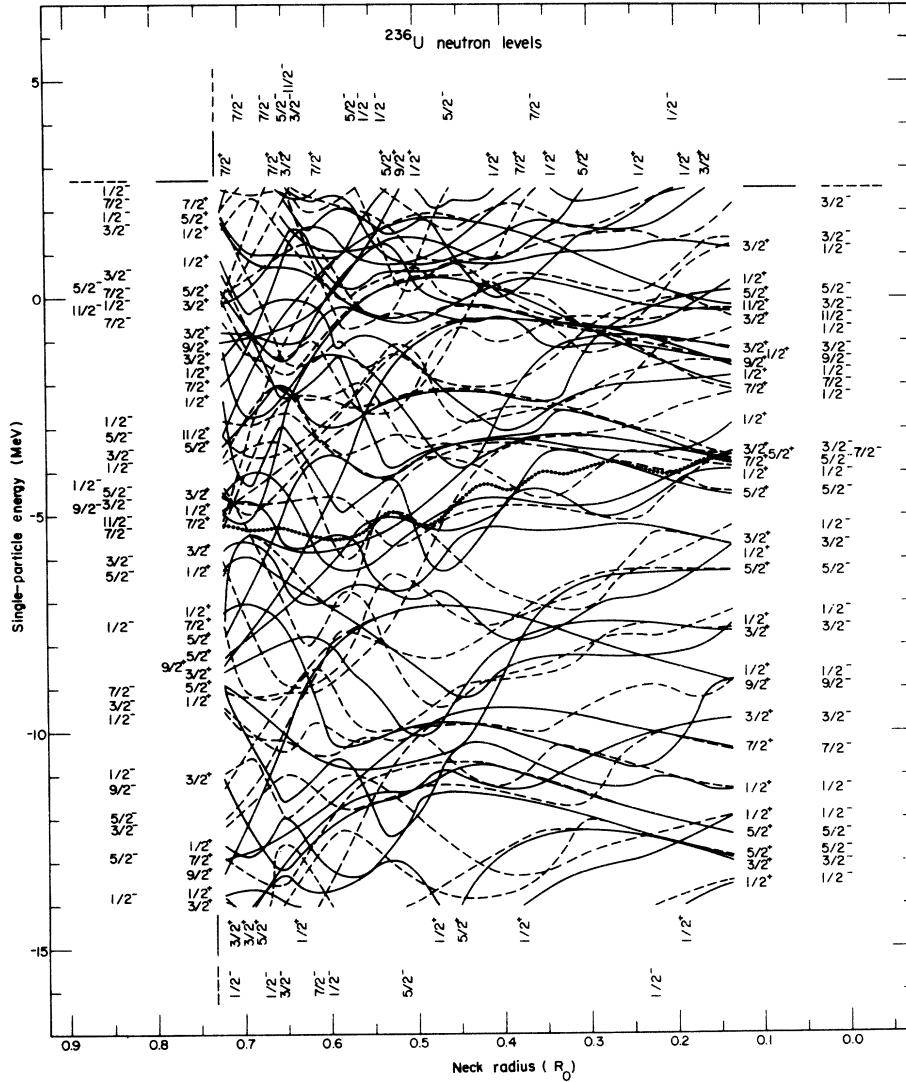


FIG. 4. Single-neutron energies of ^{238}U from the saddle point onwards for the dynamical path corresponding to $\mu = 0.02$ TP. The levels are labeled by the projection Ω (or K) of the total angular momentum on the nuclear symmetry axis and by the parity. In addition, odd-parity levels are drawn dashed. The heavy dotted line gives the location of the Fermi surface. The levels are plotted versus the neck radius, in units of the radius of the spherical nucleus $R_0 = (1.16 \text{ fm}) A^{1/3} = 7.17 \text{ fm}$.

where N_p is the number of active pairs of time-reversed orbitals. This leads to pairing strengths that vary slightly with deformation but that are approximately $G_n \approx 0.09 \text{ MeV}$ for neutrons and $G_p \approx 0.12 \text{ MeV}$ for protons.

4. Integration of the pairing equations

Because the pairing equations diverge for an infinite number of active levels, a limited number N_p of levels are used in the calculations. We take $\frac{1}{2}N_p$ to be equal to the number of bound levels above the sharp Fermi surface at time $t=0$. In this way N_p

becomes 48 for neutrons and 38 for protons. Then N_p levels, with half lying above and half lying below the sharp Fermi surface, are used as the single-particle energies $\epsilon_i(t)$.

Because many levels move out of or into the region surrounding the Fermi surface, an integration of Eqs. (8) keeping track of all levels which at one time or another pass through this region would be difficult. Therefore, whenever the highest or lowest of the N_p active levels is crossed by an intruder level that is currently not being followed, we switch from the original level to the intruder level. In this way we integrate numerically equations for a

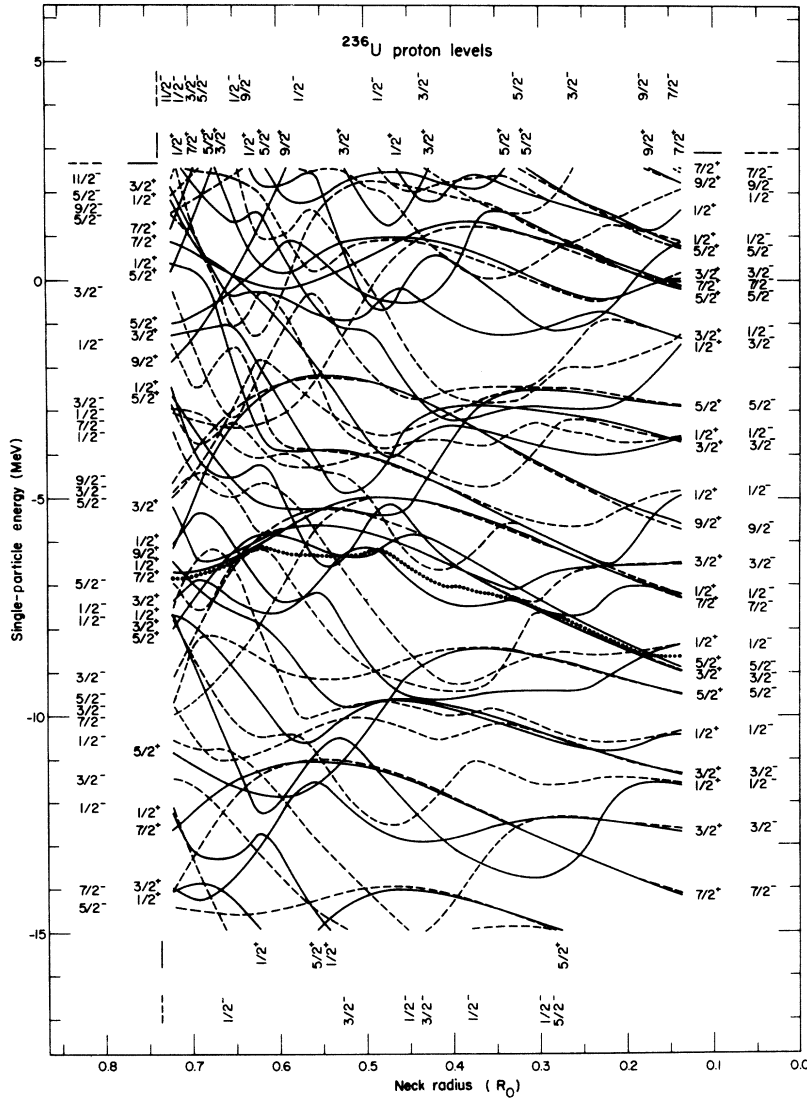


FIG. 5. Single-proton energies of ^{236}U from the saddle point onwards, analogous to Fig. 4.

constant number of levels that span an approximately constant region of energy about the sharp Fermi surface. This procedure limits excitations of the system to within about 7 MeV of the Fermi surface. It is a valid approximation as long as the levels that leave the active region carry little excitation with them, which is found to be the case in the actual calculations. As a numerical test of this approximation, we increased N_p to include all levels initially up to $\epsilon_1(0) = +2$ MeV (and an equal number below), with negligible change in the results. Some details concerning the numerical integration of the equations are discussed in Appendix C.

5. Comparison of dissipated energies

We attempt to determine the viscosity coefficient μ by requiring that the energy dissipated in the microscopic calculations equal that dissipated in the macroscopic calculations. Such a self-consistency should be possible because as the viscosity coefficient increases, the energy dissipated in the macroscopic calculations increases, whereas the slower rate of descent means that the energy dissipated in the microscopic calculations decreases.

Ideally, the determination of the viscosity coefficient in this way should not depend upon the pre-

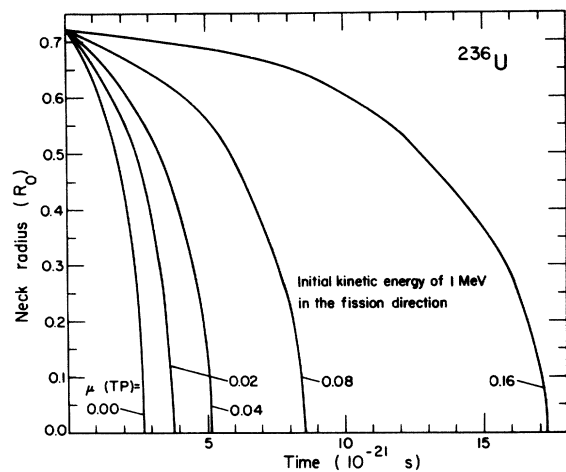


FIG. 6. Dependence of the ^{236}U neck radius upon time, for various values of the nuclear viscosity coefficient μ . The results are calculated in a macroscopic hydrodynamical model for initial conditions corresponding to starting from the saddle point with 1 MeV of kinetic energy in the fission direction.

cise position along the descent to scission at which the dissipated energies are equated. However, it turns out that the results are sensitive to this position. We therefore present our results for the viscosity coefficient as a function of the neck radius at which the comparison is made.

B. Results

Figure 7 shows the variation in the neutron and proton pairing gaps corresponding to the instantaneous static BCS ground-state solution. Here, as

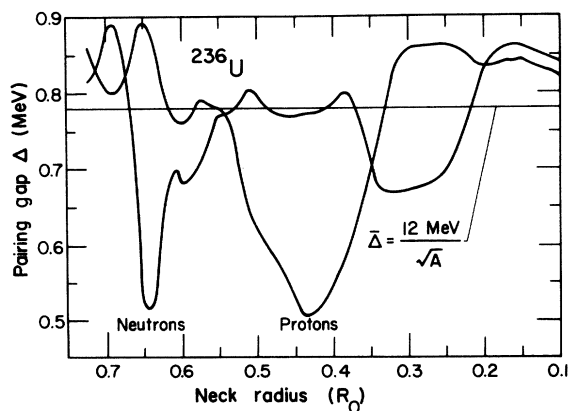


FIG. 7. Neutron and proton pairing gaps for the instantaneous static BCS ground state of ^{236}U . The results are calculated from the saddle point onwards with the single-particle levels of Figs. 4 and 5, which correspond to the hydrodynamical path for $\mu = 0.02$ TP. The horizontal line gives the average pairing gap $\bar{\Delta} = 12 \text{ MeV} / \sqrt{A} = 0.781 \text{ MeV}$ for a uniform distribution of levels.

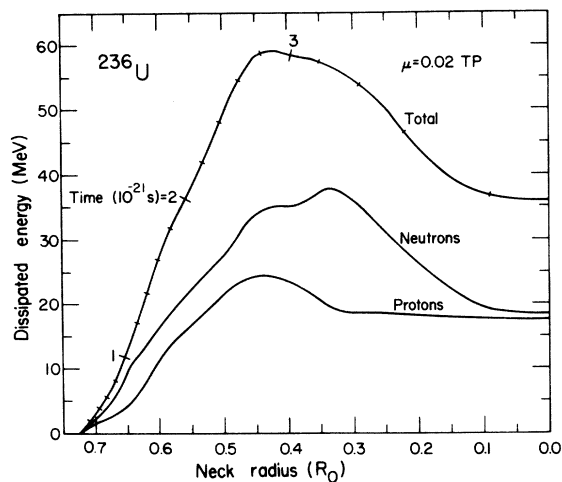


FIG. 8. Energies dissipated in the microscopic calculations as functions of the neck radius for a rate of descent corresponding to the hydrodynamical path for $\mu = 0.02$ TP. The two lower curves give the energies dissipated by the neutrons and protons separately, and the upper curve gives the total. The numbers along the upper curve give the times from the saddle point to the indicated points, in units of 10^{-21} s.

well as in the next two figures, the average pairing gap $\bar{\Delta}$ is taken equal to $12 \text{ MeV} / \sqrt{A} = 0.781 \text{ MeV}$. As can be seen by comparing Fig. 7 with Figs. 4 and 5, the maxima in the pairing gaps arise from a high density of single-particle levels near the Fermi surface, and the minima arise from a low density of levels.

In Fig. 8 we show the energy dissipated microscopically for a rate of descent corresponding to the macroscopic hydrodynamical path for $\mu = 0.02$ TP. The individual contributions from the neutrons and protons, as well as the total, are shown. The total dissipated energy goes through a maximum value of 59 MeV at a neck radius of $0.42R_0$ and then decreases.

The energy dissipated by the neutrons peaks somewhat later than that dissipated by the protons. As can be seen by comparing Figs. 7 and 8, the maxima in the energies dissipated by the neutrons and protons are correlated with the minima in the neutron and proton pairing gaps at neck radii of $0.33R_0$ and $0.44R_0$, respectively.

The maxima in the dissipated energies arise because the character of the ground-state solution is changing so rapidly that the system cannot adjust itself. Thus, the system appears excited not because of any large changes in the occupation amplitudes, but because of changes in the ground state to which the dynamic state is compared. However, only a portion of the excitation energy can be accounted for by changes in the pairing gap Δ . Even at shapes where $\Delta(t)$ is relatively constant, the ex-

citation energy $E^*(t)$ continues to rise initially because of changes in the single-particle levels $\epsilon_i(t)$. Also, for larger values of the pairing gap the energy continues to rise initially, although it is now much less sensitive to the detailed variation of Δ .

The solid curves in Fig. 9 show the total energy dissipated microscopically along the path from saddle to scission for four different rates of descent. As expected, the dissipated energy decreases as the rate of descent decreases. All curves display a broad peak followed by a relaxation; the latter is less pronounced for the slower paths (larger values of μ). The ratio between the neutron and proton contributions to the dissipated energy changes significantly with the rate of descent; it is 1.5 at the peak of the $\mu = 0.02$ TP curve and rises to 4 at the peak of the $\mu = 0.16$ TP curve.

From these results we see that our microscopic calculations reproduce a macroscopic description of energy dissipation in the sense that slowly moving systems become less excited than rapidly moving ones. However, macroscopic irreversibility is not borne out in the microscopic calculations. In particular, the relaxation in the dissipated energies indicates fluctuations on a microscopic scale that violate macroscopic irreversibility.

The similarity of the curves in Fig. 9 for the two faster rates of descent permits us to estimate numerically the maximum possible contribution to the dissipated energies from collective effects. Let us assume that when the neck radius equals $0.42R_0$, which corresponds to the shape for which the $\mu = 0$ curve has its maximum value, the energies shown

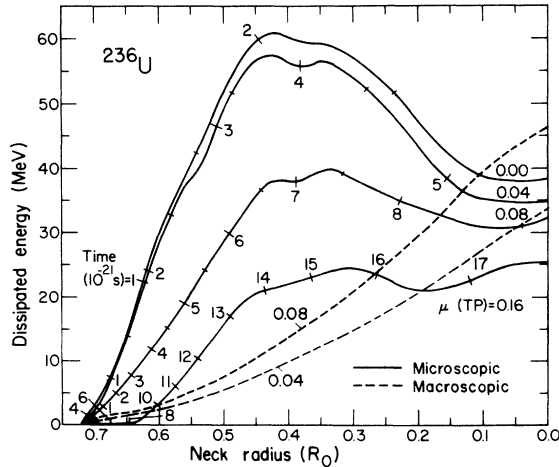


FIG. 9. Comparison of energy dissipated in the microscopic calculations (solid curves) with that dissipated in the macroscopic calculations (dashed curves), for various rates of descent specified by the values of the viscosity coefficient μ . The numbers along the solid curves give the times from the saddle point to the indicated points in units of 10^{-21} s.

in the figure actually consist of both dissipated energy and collective kinetic energy. At this point the difference in energy between the $\mu = 0$ curve (which we designate by rapid) and the $\mu = 0.04$ TP curve (which we designate by slow) is 3.5 MeV, which means that

$$E_{\text{rapid}}^* - E_{\text{slow}}^* + E_{\text{rapid}}^{\text{kin}} - E_{\text{slow}}^{\text{kin}} = 3.5 \text{ MeV.}$$

Because the excitation energy E_{rapid}^* for the rapid descent must be greater than the excitation energy E_{slow}^* for the slow descent, it follows that the collective kinetic energies for the two rates of descent satisfy the inequality (the two inertias should be approximately equal)

$$E_{\text{rapid}}^{\text{kin}} - E_{\text{slow}}^{\text{kin}} = E_{\text{rapid}}^{\text{kin}} \left[1 - \left(\frac{v_{\text{slow}}}{v_{\text{rapid}}} \right)^2 \right] < 3.5 \text{ MeV.}$$

Upon inserting values for the collective velocities v_{slow} and v_{rapid} obtained from the slopes at $0.42R_0$ of the curves in Fig. 6, we are led finally to the important result that

$$E_{\text{rapid}}^{\text{kin}} < 5.1 \text{ MeV.}$$

Thus, for our most rapid rate of descent the collective kinetic energy at this point is less than 5.1 MeV out of 61.0 MeV, or less than 8%.

The dashed curves in Fig. 9 show the corresponding energy dissipated in the macroscopic calculations for two different values of the viscosity coefficient. It is seen that at zero neck radius the energy dissipated in the two approaches is equal for a viscosity coefficient of 0.04 TP. This can also be seen from Fig. 10, where the final dissipated ener-

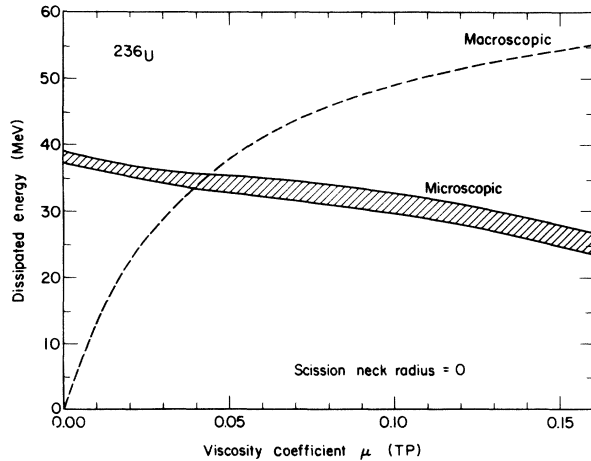


FIG. 10. Comparison of energy dissipated at zero neck radius in the microscopic calculations (hatched region) with that dissipated in the macroscopic calculations (dashed curve), as a function of the rate of descent specified by the viscosity coefficient μ . The lower boundary of the microscopic calculations corresponds to an average pairing gap $\bar{\Delta}$ of $13 \text{ MeV}/\sqrt{A}$, and the upper boundary to $11 \text{ MeV}/\sqrt{A}$.

gies at zero neck radius are plotted as functions of the viscosity coefficient. The hatched region in Fig. 10 and in the next two figures corresponds to a variation in the average pairing gap $\bar{\Delta}$ from 11 MeV/ \sqrt{A} to 13 MeV/ \sqrt{A} .

The above procedure of requiring that at the scission point the energy dissipated in the microscopic calculations equal that dissipated in the macroscopic calculations leads to 34 MeV of dissipated energy. This is almost twice the value of 18 MeV obtained from macroscopic hydrodynamical calculations that reproduce experimental fission-fragment kinetic energies.^{5,6} For our macroscopic model that takes into account the finite range of the nuclear force, the total energy decrease from the saddle point to scission for the nonviscous descent of ^{236}U is 53 MeV, whereas in the pure liquid-drop model it is 35 MeV.⁹⁰

In the fission of an actual nucleus, the neck is expected to rupture somewhat before it reaches zero radius. A simple estimate yields a neck radius of about 1.2 fm = 0.17 R_0 at which the attractive nuclear force can no longer withstand the repulsive Coulomb force.⁹¹ As shown in Fig. 11, when this scission neck radius is used to compare the energies dissipated in the two approaches, one obtains a larger viscosity coefficient of about 0.08 TP. Finally, in Fig. 12 we show how the deduced value of the viscosity coefficient depends upon the scission neck radius at which the dissipated energies are compared. These values are all considerably larger than the value of 0.015 ± 0.005 TP obtained from a comparison of calculated and experimental fission-fragment kinetic energies.

We have investigated the sensitivity of our results to the prescription used to calculate the pairing strength $G(t)$ by performing additional calculations with a constant value of G . When G is held constant at its saddle-point value corresponding to an average pairing gap $\bar{\Delta}$ of 12 MeV/ \sqrt{A} , the results differ from those of Figs. 8 and 9 by less than 0.5 MeV. It is also possible to invert the relationship between the pairing forces and viscosity and ask what value of $\bar{\Delta}$ is required to reproduce the viscosity coefficient obtained from the comparison with experimental fission-fragment kinetic energies. We find that in order to reproduce the upper limit of 0.02 TP obtained in this way, the average pairing gap $\bar{\Delta}$ must be approximately 30 MeV/ \sqrt{A} , or about 2.5 times the usual value. However, because of the exponential dependence of the pairing gap Δ on the pairing strength G , the corresponding increase in the average pairing strength G is only about 0.05 MeV, or some 50%. This represents an increase in the neutron pairing gap G_n from about 0.09 to 0.14 MeV, and in the proton pairing gap G_p from about 0.12 to 0.17 MeV.

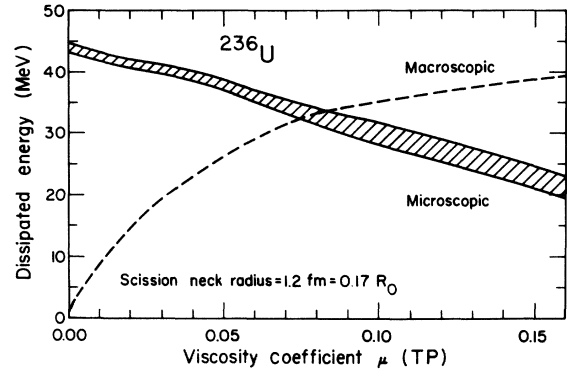


FIG. 11. Comparison of dissipated energies at a neck radius of 1.2 fm, analogous to Fig. 10.

C. Discussion

Why is the viscosity coefficient determined from the microscopic calculations larger than that determined from the macroscopic calculations? One possible answer is that the residual interaction felt by two pairs of nearly degenerate particles is somewhat larger than the average pairing strength G , which would reduce the value of the viscosity coefficient obtained from the microscopic approach. Although many important nuclear properties can be described adequately in terms of a constant average

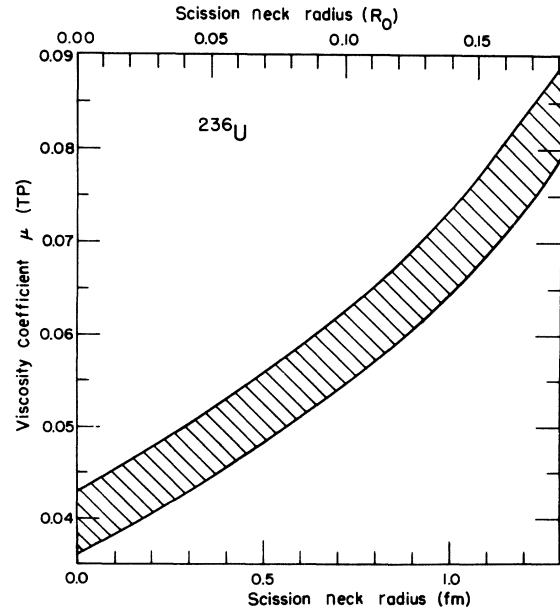


FIG. 12. Dependence of the viscosity coefficient upon the value of the neck radius at which the dissipated energies are compared. The lower boundary corresponds to an average pairing gap $\bar{\Delta}$ of 13 MeV/ \sqrt{A} , and the upper boundary to 11 MeV/ \sqrt{A} .

pairing interaction acting between a given number of pairs of particles, nuclear dissipation depends primarily upon the level splitting between nearly degenerate pairs of particles, and consequently may not be describable in terms of a constant pairing interaction.

Although for a δ -function residual interaction it is not true that the matrix elements for nearby levels are larger than those for well-separated levels,^{92,93} it is possible that this could be the case for a realistic residual interaction of finite range.⁹⁴

It is also possible that for the very deformed shapes encountered in fission the pairing strength G should be larger than the ground-state value that we have used. The early interpretations of fission-fragment angular-distribution data that suggested that the pairing gap increases with deformation are now in doubt,⁹⁵ and the theoretical studies that suggest that the pairing strength should be proportional to the surface area⁹⁶ are inconclusive. Nevertheless, in order to reproduce the larger average pairing gap $\bar{\Delta}$ in the fission fragments compared to that of the original system, it is necessary for the value of G to increase by about 14% when all the levels of the system are considered. This is much less than the 50% increase required to reduce the dissipated energy to the upper limit obtained in the macroscopic calculations.

An even more important effect is that the character of the pairing force should vary with the shape of the system. Specifically, when the two fragments have almost separated, states paired in one fragment should not be coupled to states paired in the other fragment. Thus, $G(t)$ should be a matrix, varying in time so as to allow such decoupling to increase as the fragments separate.^{92,97}

The value of $\mu = 0.015 \pm 0.005$ TP that was determined by comparing macroscopic hydrodynamical calculations with experimental fission-fragment kinetic energies is an average value appropriate to the fission of highly excited nuclei, whereas our microscopic calculations are performed for initial conditions corresponding to an unexcited BCS ground state at the saddle point. However, for initial conditions corresponding to a highly excited nucleus at the saddle point, the energy dissipated microscopically should be even larger than in the present calculations because the pairing interaction is not effective between broken pairs of nucleons.

Possible mechanisms for increasing the effective splitting at level crossings are axially asymmetric (γ) and reflection-asymmetric (mass-asymmetric) vibrations of the nucleus as it descends from the saddle point to scission. If the most probable shape during the descent is symmetric the most probable level splittings are zero, but the finite root-mean-

square deviations from axial and reflection symmetry lead to finite root-mean-square values of the level splittings. Of course, for those nuclei whose most probable shapes during the descent are reflection asymmetric, the degeneracies of levels characterized by the same value of Ω are split by this asymmetry alone. Similarly, axially asymmetric vibrations alone suffice to split the degeneracies for states of identical parity.

An additional contribution to the splitting is provided by the coupling between the fission degree of freedom and these asymmetric degrees of freedom. This coupling should cause the nucleus to avoid regions of near degeneracy and hence high dissipation (as well as high potential energy and high inertia) during its dynamical descent. It remains an important problem for the future to calculate the dissipation from saddle to scission for a nucleus with axially asymmetric and reflection-asymmetric degrees of freedom.

However, there are other possibilities that would reduce the value of the viscosity coefficient obtained from the microscopic approach. For example, our separation procedure has not removed all of the collective energy from $E^*(t)$. We have seen that in the limiting case of zero pairing $E^*(t)$ contains only small contributions from collective effects. Also, we showed numerically that in the presence of pairing the contribution from the collective kinetic energy is less than 5.1 MeV or 8% at the peak in the dissipated energy for rapid descents. It is also possible that a portion of $E^*(t)$ is not macroscopically irreversible and hence is not true internal excitation energy. Both of these points clearly demand further study.

It is also possible that the true nuclear inertia may be sufficiently larger than the nearly irrotational value that we have used to reduce substantially the rate of descent. It is well known that nuclear flow is not irrotational for ground-state vibrational motion and for the adiabatic penetration of the fission barrier in spontaneous fission.² However, at larger distortions the single-particle levels do not vary as rapidly with deformation, and at higher internal excitations the energy denominators in the cranking formula for the inertia^{2,82} are no longer all of one sign. Both of these effects reduce the size of the calculated inertias, and for these cases the assumption of irrotational flow should be somewhat better.

Finally, starting the system with less than 1 MeV of kinetic energy in the fission direction would decrease somewhat the rate of descent and hence the energy dissipation. The initial kinetic energy E_f in the fission direction is of course not a specific value but is a distribution of values. At high excitation energies, where classical statistical me-

chanics becomes valid, the values of E_f are distributed according to the Boltzmann factor $\exp(-E_f/\Theta)$, where Θ is the nuclear temperature.⁸⁴ The initial value $E_f = 1$ MeV is therefore a typical value for high excitation energies. Although the initial energy dissipation depends upon E_f , the dissipation during the later stages is relatively insensitive to this quantity.

At the other extreme, there are some possibilities that would increase the value of the viscosity coefficient obtained from the macroscopic approach. For example, the rupture of the neck somewhat before it reaches zero radius increases somewhat the calculated fission-fragment kinetic energies and hence increases the viscosity coefficient required to reproduce experimental values. However, use of the estimate of 1.2 fm for the neck radius at which the attractive nuclear force can no longer withstand the repulsive Coulomb force increases the viscosity coefficient μ by only 0.002 TP or 13%.⁹¹

At low excitation energies single-particle effects can increase the kinetic energy relative to that calculated for a macroscopic potential energy and hence increase the viscosity coefficient required to reproduce experimental values. But single-particle effects are expected to disappear at the higher excitation energies involved in the determination of the viscosity coefficient by comparing experimental fission-fragment kinetic energies with calculated values.

Finally, it is possible that the shape dependence of the viscosity tensor is different from that calculated for macroscopic hydrodynamical flow. In particular, it has been suggested⁹⁸ that Landau damping, in which the excitation of nucleons proceeds by means of one-body collisions with a moving potential wall²⁷ rather than through two-body collisions with other nucleons, could lead to a viscosity tensor in which neck formation is enhanced rather than hindered. If this were the case, calculated fission-fragment kinetic energies could remain large at the experimental values even for a large viscosity coefficient. This suggestion is currently being explored.

IV. SUMMARY AND CONCLUSION

We have studied the excitation of the internal degrees of freedom of a ^{236}U nucleus as it moves from its saddle point to scission along a path determined from macroscopic hydrodynamical calculations. This is done for the single-particle states in a realistic diffuse-surface potential along this path, with a residual pairing interaction. Time-dependent equations that determine the occupation probabilities were solved for different rates of de-

scension corresponding to different viscosity coefficients in the macroscopic calculations.

We attempted to determine the nuclear viscosity coefficient by requiring that the energy dissipated between the saddle point and the scission point in the microscopic calculations equal that dissipated in the macroscopic hydrodynamical calculations. This procedure led to a viscosity coefficient of 0.04 TP, which is substantially larger than the value of 0.015 ± 0.005 TP determined from macroscopic hydrodynamical calculations that reproduce experimental fission-fragment kinetic energies. The viscosity coefficient determined from the microscopic calculations is even larger if the dissipated energies are compared at a finite scission neck radius.

We discussed several possibilities for resolving this discrepancy. To us the most likely explanation is that during the descent from the saddle point to scission axially asymmetric and reflection-asymmetric deformations provide additional splittings at level crossings and hence reduce the energy dissipation. Thus, whereas in the absence of level splittings nuclei would be very viscous, we propose that the level splittings arising from axially asymmetric and reflection-asymmetric deformations make nuclei only moderately viscous. It remains an important problem for the future to check this suggestion by means of detailed calculations of energy dissipation involving these asymmetric deformations.

ACKNOWLEDGMENTS

We are grateful to R. Babinet, F. Beck, G. F. Bertsch, A. Bohr, Z. Fraenkel, J. J. Griffin, A. K. Kerman, S. J. Krieger, U. Mosel, W. D. Myers, J. W. Negele, S. G. Nilsson, A. J. Sierk, W. J. Swiatecki, and L. Wilets for stimulating discussions concerning this work, to T. A. Tombrello for suggesting the scaling procedure for the single-particle energies, and to K. T. R. Davies for providing us with the hydrodynamical paths. In addition, S. E. Koonin thanks the Los Alamos Scientific Laboratory for its support and hospitality, and J. R. Nix thanks the Aspen Center for Physics for its hospitality during the completion of this manuscript.

APPENDIX A: DETAILS IN THE DERIVATION OF THE TIME-DEPENDENT PAIRING EQUATIONS

In this Appendix we derive Eqs. (4), the time-dependent pairing equations. By use of Heisenberg's form of the equations of motion, the total time derivatives of Eqs. (3) are given by

$$i\dot{\rho}_{ij} = \langle [a_i^\dagger a_j, H] \rangle + i \left\langle \frac{\partial}{\partial t} (a_i^\dagger a_j) \right\rangle \quad (\text{A1a})$$

and

$$i\dot{\kappa}_{ij} = \langle [a_i a_{-j}, H] \rangle + i \left\langle \frac{\partial}{\partial t} (a_i a_{-j}) \right\rangle. \quad (\text{A1b})$$

(The use of the same symbol i to denote $\sqrt{-1}$ and a matrix index should cause no confusion.) Because the single-particle states are time dependent, the Fermion creation and destruction operators must be differentiated as well.

With the Hamiltonian (2), the commutator terms become

$$[a_i^\dagger a_j, H] = a_i^\dagger a_j (\epsilon_j - \epsilon_i) + G \sum_{k>0}' (a_i^\dagger a_{-j}^\dagger a_k a_{-k} + a_{-k}^\dagger a_k^\dagger a_j a_{-i}) \quad (\text{A2a})$$

and

$$[a_i a_{-j}, H] = a_i a_{-j} (\epsilon_j + \epsilon_i) - G \sum_{k>0}' (a_{-j}^\dagger a_{-i}^\dagger a_k a_{-k} - a_j a_i^\dagger a_k a_{-k}). \quad (\text{A2b})$$

The partial-derivative terms are

$$\frac{\partial}{\partial t} (a_i^\dagger a_j) = \sum_{k>0}' (a_i^\dagger a_k D_{kj} - D_{ik} a_k^\dagger a_j) \quad (\text{A3a})$$

and

$$\frac{\partial}{\partial t} (a_{-i} a_j) = \sum_{k>0}' (a_{-i} a_k D_{kj} - D_{ik} a_{-k} a_j), \quad (\text{A3b})$$

where the real antisymmetric matrix D is defined by Eq. (5); we use the fact that $D_{-i, -j} = D_{ij}$.

In taking the expectation value of Eqs. (A2), we encounter terms such as $\langle a^\dagger a a a \rangle$ and $\langle a^\dagger a^\dagger a a \rangle$, which are factorized in the usual BCS manner, e.g.

$$\begin{aligned} \langle a_i^\dagger a_{-j}^\dagger a_k a_{-k} \rangle &= \langle a_i^\dagger a_{-j}^\dagger \rangle \langle a_k a_{-k} \rangle - \langle a_i^\dagger a_k \rangle \langle a_{-j}^\dagger a_{-k} \rangle \\ &= -\kappa_{ji}^* \kappa_{kk} - \rho_{ik} \rho_{jk}. \end{aligned}$$

The assumed time-reversal symmetry of the wave function means that such terms as $\langle a_i^\dagger a_{-k} \rangle$ vanish and that the normal and time-reversed density matrices are equal.

Upon inserting Eqs. (A2) and (A3) into Eqs. (A1) we obtain

$$\begin{aligned} i\dot{\rho}_{ij} &= \rho_{ij} (\epsilon_j - \epsilon_i) \\ &- G \sum_{k>0}' (\rho_{ik} \rho_{jk} + \kappa_{ji}^* \kappa_{kk} - \rho_{ki} \rho_{kj} - \kappa_{kk}^* \kappa_{ij}) \\ &+ i \sum_{k>0}' (\rho_{ik} D_{kj} - D_{ik} \rho_{kj}) \end{aligned}$$

and

$$\begin{aligned} i\dot{\kappa}_{ij} &= \kappa_{ij} (\epsilon_i + \epsilon_j) \\ &- G \sum_{k>0}' [\rho_{jk} \kappa_{ik} - \rho_{ji} \kappa_{kk} - (\rho_{ij} - \delta_{ij}) \kappa_{kk} + \rho_{ik} \kappa_{kj}] \\ &+ \sum_{k>0}' (\kappa_{ik} D_{kj} - D_{ik} \kappa_{kj}), \end{aligned}$$

which, when written in matrix notation, become Eqs. (4).

APPENDIX B: DETERMINATION OF THE RPA MODES

We linearize Eqs. (8) about the BCS ground state in order to obtain the RPA modes. The time-dependent quantities ρ and κ are treated as vectors of dimension N_p , where N_p is the number of pairs of levels participating in the pairing force. Upon writing

$$\rho_j(t) = \bar{v}_j^2 + \delta\rho_j(t)$$

and

$$\kappa_j(t) = [\bar{u}_j \bar{v}_j + \delta\kappa_j(t)] \exp[-i(2\lambda - G)t],$$

Eqs. (8) yield, to first order in $\delta\rho$ and $\delta\kappa$,

$$\frac{d\delta\rho}{dt} = 2\Delta \text{Im}\delta\kappa - 2G\bar{u}\bar{v}Q \text{Im}\delta\kappa$$

and

$$\frac{d\delta\kappa}{dt} = -2i(\eta + GnQ)\delta\kappa - 2i(\Delta - G\bar{u}\bar{v})\delta\rho.$$

The matrices \bar{u} , \bar{v} , n , η , and Q are defined in Eqs. (20) and in the lines that follow them.

We assume harmonic time variations for $\delta\rho$ and $\delta\kappa$, namely,

$$\delta\rho(t) = \delta\rho_c \cos\omega t + \delta\rho_s \sin\omega t$$

and

$$\delta\kappa(t) = \delta\kappa_+ \exp(i\omega t) + \delta\kappa_- \exp(-i\omega t),$$

where $\delta\rho_c$ and $\delta\rho_s$ are real. After equating positive and negative frequency components, we obtain

$$\omega\delta\rho_c = -2(\Delta - G\bar{u}\bar{v}Q) \text{Im}(\delta\kappa_+ - \delta\kappa_-),$$

$$\omega\delta\rho_s = 2(\Delta - G\bar{u}\bar{v}Q) \text{Im}(\delta\kappa_+ + \delta\kappa_-),$$

$$\omega\delta\kappa_+ = -2(\eta + GnQ)\delta\kappa_+ - (\Delta - G\bar{u}\bar{v})(\delta\rho_c - i\delta\rho_s),$$

and

$$\omega\delta\kappa_- = 2(\eta + GnQ)\delta\kappa_- + (\Delta - G\bar{u}\bar{v})(\delta\rho_c + i\delta\rho_s).$$

Under the assumption that ω is real, these may be solved to yield the eigenvalue equation

$$\begin{aligned} \frac{1}{4}\omega^2 \text{Im}(\delta\kappa_+ + \delta\kappa_-) &= [(\eta + GnQ)^2 + (\Delta - G\bar{u}\bar{v})(\Delta - G\bar{u}\bar{v}Q)] \text{Im}(\delta\kappa_+ + \delta\kappa_-) \\ &\equiv T \text{Im}(\delta\kappa_+ + \delta\kappa_-). \end{aligned} \quad (\text{B1})$$

The form of the matrix T given in Eq. (19) is obtained by expanding Eq. (B1) and by realizing that

$$G^2 n Q n Q = G^2 (\text{Tr} n) n Q = G^2 (N - \frac{1}{2} N_p) n Q.$$

APPENDIX C: NUMERICAL METHODS

Equations (8) present, for N_p active levels, a set of $2N_p$ nonlinear first-order coupled differential equations for the real quantities ρ and complex quantities κ . These equations were integrated numerically by means of a fourth-order Adams-Moulton predictor-corrector method,⁹⁹ with a Runge-Kutta starting procedure as outlined by Zonneveld.¹⁰⁰ At all times, the absolute error in all dependent variables was required to be less than 5×10^{-6} . A time grid of 5×10^{-23} s was found

to be sufficient for both neutrons ($N_n = 48$) and protons ($N_p = 38$); halving the step size gave negligible changes in the results. The integration was checked further by computing $E^*(t)$ after Eqs. (8) had been integrated an equivalent number of steps for a comparable static system (the saddle-point shape). Finally, we remark that a substantial improvement in integration efficiency was achieved by redefining the zero of the single-particle energies $\epsilon_i(t)$ so that the chemical potential $\lambda(t)$ was approximately zero, as this avoided integrating the superfluous winding phase of the pairing-field elements $\kappa_i(t)$ discussed in Sec. II B.

*This work was supported by the U. S. Energy Research and Development Administration under Contract Nos. AT(11-1)/3069 and W-7405-ENG-36.

[†]National Science Foundation Graduate Fellow. Present address: Kellogg Radiation Laboratory, California Institute of Technology, Pasadena, California 91125.

¹H. Goldstein, *Classical Mechanics* (Addison-Wesley, Reading, 1959), Chap. 1, Sec. 5, pp. 19–22.

²J. R. Nix, *Annu. Rev. Nucl. Sci.* **22**, 65 (1972).

³A. J. Sierk and J. R. Nix, in *Proceedings of the Third International Atomic Energy Agency Symposium on Physics and Chemistry of Fission, Rochester, New York, 1973* (International Atomic Energy Agency, Vienna, 1974), Vol. II, p. 273.

⁴J. R. Nix and A. J. Sierk, *Phys. Scr.* **10A**, 94 (1974).

⁵K. T. R. Davies, S. E. Koonin, J. R. Nix, and A. J. Sierk, in *Proceedings of the International Workshop III on Gross Properties of Nuclei and Nuclear Excitations*, Hirschegg, Kleinwalsertal, Austria, 1975 [Technische Hochschule Darmstadt Report No. AED-Conf-75-009-000, 1975 (unpublished)], p. 8.

⁶K. T. R. Davies, A. J. Sierk, and J. R. Nix, Los Alamos Scientific Laboratory report (unpublished).

⁷J. Schirmer, S. Knaak, and G. Süssmann, *Nucl. Phys.* **A199**, 31 (1973).

⁸R. Wierzch, R. W. Hasse, and G. Süssmann, in *Proceedings of the Third International Atomic Energy Agency Symposium on Physics and Chemistry of Fission, Rochester, New York, 1973* (see Ref. 3), Vol. I, p. 523.

⁹R. Wierzch, R. W. Hasse, and G. Süssmann, in *Proceedings of the International Conference on Nuclear Physics, Munich, Germany, 1973*, edited by J. de Boer and H. J. Mang (North-Holland, Amsterdam/American Elsevier, New York, 1973), Vol. 1, p. 585.

¹⁰R. W. Hasse, in *Proceedings of the International Workshop III on Gross Properties of Nuclei and Nuclear Excitations*, Hirschegg, Kleinwalsertal, Austria, 1975 (see Ref. 5), p. 22.

¹¹C. T. Alonso, Lawrence Berkeley Laboratory Report No. LBL-2993, 1974 (unpublished).

¹²W. J. Swiatecki, in *Proceedings of the International Conference on Nuclear Reactions Induced by Heavy Ions, Heidelberg, Germany, 1969*, edited by R. Bock and W. R. Hering (North-Holland, Amsterdam/American Elsevier, New York, 1970), p. 729.

¹³W. J. Swiatecki and S. Björnholm, *Phys. Rep.* **4C**, 325 (1972).

¹⁴W. J. Swiatecki, *J. Phys. Suppl.* **33**, C5-45 (1972).

¹⁵S. Björnholm, *Phys. Scr.* **10A**, 110 (1974).

¹⁶H. Nifenecker, C. Signarbieux, R. Babinet, and J. Poitou, in *Proceedings of the Third International Atomic Energy Agency Symposium on Physics and Chemistry of Fission, Rochester, New York, 1973* (see Ref. 3), Vol. II, p. 117.

¹⁷P. Armbruster, in *Proceedings of the International Workshop III on Gross Properties of Nuclei and Nuclear Excitations*, Hirschegg, Kleinwalsertal, Austria, 1975 (see Ref. 5), p. 32.

¹⁸H. Schultheis and R. Schultheis, in *Proceedings of the XIII International Winter Meeting on Nuclear Physics, Bormio, Italy, 1975* [University of Milan report, 1975 (unpublished)], p. 44.

¹⁹H. Schultheis and R. Schultheis, *Phys. Lett.* **57B**, 7 (1975).

²⁰W. D. Myers, in *Proceedings of the International Conference on Reactions between Complex Nuclei, Nashville, Tennessee, 1974*, edited by R. L. Robinson, F. K. McGowan, J. B. Ball, and J. H. Hamilton (North-Holland, Amsterdam/American Elsevier, New York, 1974), Vol. 2, p. 1.

²¹D. H. E. Gross, H. Kalinowski, and R. Beck, in *Proceedings of the International Conference on Nuclear Physics, Munich, Germany, 1973* (see Ref. 9), Vol. 1, p. 394.

²²R. Beck and D. H. E. Gross, *Phys. Lett.* **47B**, 143 (1973).

²³D. H. E. Gross and H. Kalinowski, *Phys. Lett.* **48B**, 302 (1974).

²⁴D. H. E. Gross and H. Kalinowski, in *Proceedings of the International Conference on Reactions between Complex Nuclei, Nashville, Tennessee, 1974* (see Ref. 20), Vol. 1, p. 118.

²⁵D. H. E. Gross, H. Kalinowski, and J. N. De, in *Proceedings of the Symposium on Classical and Quantum Mechanical Aspects of Heavy Ion Collisions, Heidelberg, Germany, 1974*, edited by H. L. Harney, P. Braun-Munzinger, and C. L. Gelbke (Springer-Verlag, Berlin, 1975), p. 194.

²⁶D. H. E. Gross, J. N. De, and H. Kalinowski, in *Proceedings of the International Workshop III on Gross Properties of Nuclei and Nuclear Excitations*, Hirschegg,

- Kleinwalsertal, Austria, 1975 (see Ref. 5), p. 129.
- ²⁷D. H. E. Gross, Nucl. Phys. A240, 472 (1975).
- ²⁸J. Wilczyński, Phys. Lett. 47B, 484 (1973).
- ²⁹J. P. Bondorf, M. I. Sobel, and D. Sperber, in *Proceedings of the International Conference on Reactions between Complex Nuclei, Nashville, Tennessee, 1974* (see Ref. 20), Vol. 1, p. 132.
- ³⁰J. P. Bondorf, in *Proceedings of the International Conference on Reactions between Complex Nuclei, Nashville, Tennessee, 1974* (see Ref. 20), Vol. 2, p. 383.
- ³¹J. P. Bondorf, Deeply Inelastic Heavy Ion Reactions, Proceedings of the International School of Physics "Enrico Fermi," Course LXII [Academic, New York (to be published)].
- ³²D. Sperber, Phys. Scr. 10A, 115 (1974).
- ³³J. P. Bondorf, M. I. Sobel, and D. Sperber, Phys. Rep. 15C, 83 (1974).
- ³⁴J. P. Bondorf, J. R. Huizenga, M. I. Sobel, and D. Sperber, Phys. Rev. C 11, 1265 (1975).
- ³⁵C. F. Tsang, Phys. Scr. 10A, 90 (1974).
- ³⁶R. H. Davis, in *Proceedings of the International Conference on Reactions between Complex Nuclei, Nashville, Tennessee, 1974* (see Ref. 20), Vol. 1, p. 125.
- ³⁷R. H. Davis, Phys. Rev. C 9, 2411 (1974).
- ³⁸R. H. Davis, Florida State University report, 1974 (unpublished).
- ³⁹R. H. Davis, in Proceedings of the International Symposium on Cluster Structure of Nuclei and Transfer Reactions Induced by Heavy Ions, Tokyo, Japan, 1975 (unpublished).
- ⁴⁰F. Beck, in Proceedings of the International Workshop III on Gross Properties of Nuclei and Nuclear Excitations, Hirschegg, Kleinwalsertal, Austria, 1975 (see Ref. 5), p. 135.
- ⁴¹F. Beck, Lawrence Berkeley Laboratory report (unpublished).
- ⁴²H. H. Deubler and K. Dietrich, Phys. Lett. 56B, 241 (1975).
- ⁴³C. Y. Wong, Oak Ridge National Laboratory report, 1975 (unpublished).
- ⁴⁴G. Wegmann, Phys. Lett. 50B, 327 (1974).
- ⁴⁵G. Wegmann, in Proceedings of the International Workshop III on Gross Properties of Nuclei and Nuclear Excitations, Hirschegg, Kleinwalsertal, Austria, 1975 (see Ref. 5), p. 28.
- ⁴⁶C. Toepffer, in *Proceedings of the International Conference on Reactions between Complex Nuclei, Nashville, Tennessee, 1974* (see Ref. 20), Vol. 1, p. 129; in *Proceedings of the Symposium on Classical and Quantum Mechanical Aspects of Heavy Ion Collisions, Heidelberg, Germany, 1974* (see Ref. 25), p. 15.
- ⁴⁷A. K. Kerman and S. E. Koonin, Phys. Scr. 10A, 118 (1974).
- ⁴⁸H. Hofmann, in Proceedings of the XIII International Winter Meeting on Nuclear Physics, Bormio, Italy, 1975 (see Ref. 18), p. 94.
- ⁴⁹H. Hofmann and P. J. Siemens, Niels Bohr Institute report, 1975 (unpublished).
- ⁵⁰J. D. Immele, in *Proceedings of the International Conference on Nuclear Physics, Munich, Germany, 1973* (see Ref. 9), Vol. 1, p. 584.
- ⁵¹J. J. Griffin and K. K. Kan, in *Proceedings of the Third International Atomic Energy Agency Symposium on Physics and Chemistry of Fission, Rochester, New York, 1973* (see Ref. 3), Vol. I, p. 533; in Proceedings of the International Workshop III on Gross Properties of Nuclei and Nuclear Excitations, Hirschegg, Kleinwalsertal, Austria, 1975 (see Ref. 5), p. 56.
- ⁵²K. K. Kan and J. J. Griffin, in *Proceedings of the International Conference on Reactions between Complex Nuclei, Nashville, Tennessee, 1974* (see Ref. 20), Vol. 1, p. 127; Phys. Lett. 50B, 241 (1974); K.K. Kan, Ph.D. thesis, University of Maryland, 1975 (unpublished).
- ⁵³J. D. Immele, K. K. Kan, and J. J. Griffin, Nucl. Phys. A241, 47 (1975).
- ⁵⁴L. G. Moretto and J. S. Sventek, Lawrence Berkeley Laboratory Report No. LBL-3443, 1974 (unpublished).
- ⁵⁵W. Nörenberg, in *Proceedings of the International Conference on Reactions between Complex Nuclei, Nashville, Tennessee, 1974* (see Ref. 20), Vol. 1, p. 90; Phys. Lett. 52B, 289 (1974); in Proceedings of the International Workshop III on Gross Properties of Nuclei and Nuclear Excitations, Hirschegg, Kleinwalsertal, Austria, 1975 (see Ref. 5), p. 50; Z. Phys. (to be published).
- ⁵⁶R. W. Hasse, J. Math. Phys. 16, 2005 (1975).
- ⁵⁷B. Giraud, Tools for a Theory of Reactions between Heavy Ions, Proceedings of the International School of Physics "Enrico Fermi," Course LXII [Academic, New York (to be published)].
- ⁵⁸B. Giraud, J. Le Tourneux, and E. Osnes, Phys. Rev. C 11, 82 (1975).
- ⁵⁹R. A. Broglia, C. H. Dasso, and A. Winther, Phys. Lett. 53B, 301 (1974).
- ⁶⁰G. F. Bertsch, Los Alamos Scientific Laboratory Report No. LA-UR-75-479, 1975 (unpublished).
- ⁶¹C. Y. Wong, J. A. Maruhn, and T. A. Welton, Oak Ridge National Laboratory report, 1975 (unpublished).
- ⁶²D. L. Hill and J. A. Wheeler, Phys. Rev. 89, 1102 (1953).
- ⁶³J. J. Griffin, in *Proceedings of the Second International Atomic Energy Agency Symposium on Physics and Chemistry of Fission, Vienna, Austria, 1969* (International Atomic Energy Agency, Vienna, 1969), p. 3; Nucl. Phys. A170, 395 (1971).
- ⁶⁴L. Wilets, *Theories of Nuclear Fission* (Clarendon, Oxford, 1964), Chap. 5, pp. 89-100.
- ⁶⁵G. Schütte and L. Wilets, in *Proceedings of the Third International Atomic Energy Agency Symposium on Physics and Chemistry of Fission, Rochester, New York, 1973* (see Ref. 3), Vol. I, p. 503.
- ⁶⁶G. Schütte and L. Wilets, Nucl. Phys. (to be published).
- ⁶⁷Y. Boneh, Z. Fraenkel, and Z. Paltiel, in *Proceedings of the Third International Atomic Energy Agency Symposium on Physics and Chemistry of Fission, Rochester, New York, 1973* (see Ref. 3), Vol. I, p. 515; Y. Boneh and Z. Fraenkel, Phys. Rev. C 10, 893 (1974).
- ⁶⁸T. Ledergerber, Z. Paltiel, H. C. Pauli, G. Schütte, Y. Yariv, and Z. Fraenkel, Phys. Lett. 56B, 417 (1975).
- ⁶⁹D. Glas, U. Mosel, K. H. Passler, and P. G. Zint, in Proceedings of the XII International Winter Meeting on Nuclear Physics, Villars, Switzerland, 1974 [University of Milan report, 1974 (unpublished)], p. 1.
- ⁷⁰D. Glas and U. Mosel, in *Proceedings of the International Conference on Reactions between Complex Nuclei, Nashville, Tennessee, 1974* (see Ref. 20), Vol. 1, p. 121.
- ⁷¹D. Glas and U. Mosel, Phys. Lett. 49B, 301 (1974).

- ⁷²U. Mosel and D. Glas, in *Proceedings of the International Workshop III on Gross Properties of Nuclei and Nuclear Excitations*, Hirscheegg, Kleinwalsertal, Austria, 1975 (see Ref. 5), p. 36.
- ⁷³L. Landau, *Phys. Z. Sowjetunion* **1**, 88 (1932).
- ⁷⁴L. Landau, *Phys. Z. Sowjetunion* **2**, 46 (1932).
- ⁷⁵C. Zener, *Proc. R. Soc. London, Ser. A* **137**, 696 (1932).
- ⁷⁶A. deShalit and H. Feshbach, *Theoretical Nuclear Physics, Vol. I: Nuclear Structure* (Wiley, New York, 1974), Vol. I, pp. 507–572.
- ⁷⁷D. Vautherin, *Phys. Rev. C* **7**, 296 (1973).
- ⁷⁸P. Bonche, S. E. Koonin, and J. W. Negele, Massachusetts Institute of Technology Report No. MIT-CTP-507, 1975 (unpublished).
- ⁷⁹M. Baranger, *Phys. Rev.* **120**, 957 (1960); **122**, 992 (1961).
- ⁸⁰W. Ogle, S. Wahlborn, R. Piepenbring, and S. Fredriksson, *Rev. Mod. Phys.* **43**, 424 (1971).
- ⁸¹J. W. Negele, *Nucl. Phys.* **A142**, 225 (1970).
- ⁸²D. R. Inglis, *Phys. Rev.* **103**, 1786 (1956).
- ⁸³A. K. Kerman, R. D. Lawson, and M. H. Macfarlane, *Phys. Rev.* **124**, 162 (1961).
- ⁸⁴J. R. Nix, *Nucl. Phys.* **A130**, 241 (1969); Lawrence Berkeley Laboratory Report No. UCRL-17958, 1968 (unpublished).
- ⁸⁵H. J. Krappe and J. R. Nix, in *Proceedings of the Third International Atomic Energy Agency Symposium on Physics and Chemistry of Fission, Rochester, New York, 1973* (see Ref. 3), Vol. I, p. 159.
- ⁸⁶H. J. Krappe, in *Proceedings of the Symposium on Classical and Quantum Mechanical Aspects of Heavy Ion Collisions, Heidelberg, Germany, 1974* (see Ref. 25), p. 24.
- ⁸⁷M. Bolsterli, E. O. Fiset, J. R. Nix, and J. L. Norton, *Phys. Rev. C* **5**, 1050 (1972).
- ⁸⁸P. Möller, S. G. Nilsson, and J. R. Nix, *Nucl. Phys.* **A229**, 292 (1974).
- ⁸⁹A. Bohr and B. R. Mottelson, *Nuclear Structure, Vol. I: Single-Particle Motion* (Benjamin, New York, 1969), Vol. I, pp. 169–171.
- ⁹⁰A. J. Sierk and J. R. Nix, Los Alamos Scientific Laboratory report (unpublished).
- ⁹¹A. J. Sierk and J. R. Nix, Los Alamos Scientific Laboratory report (unpublished).
- ⁹²D. Glas and U. Mosel, *Nucl. Phys.* **A216**, 563 (1973); (unpublished).
- ⁹³G. F. Bertsch (unpublished).
- ⁹⁴F. Beck (personal communication).
- ⁹⁵H. C. Britt and J. R. Huizenga, *Phys. Rev. C* **9**, 435 (1974).
- ⁹⁶R. C. Kennedy, *Phys. Rev.* **144**, 804 (1966).
- ⁹⁷R. W. Hasse, *Nucl. Phys.* **A229**, 141 (1974).
- ⁹⁸W. J. Swiatecki, Lawrence Berkeley Laboratory Report No. LBL-4296, 1975 (unpublished).
- ⁹⁹L. P. Meissner, Lawrence Berkeley Laboratory Computer Center Program No. D2 BKY ZAM, 1965 (unpublished).
- ¹⁰⁰J. A. Zonneveld, *Automatic Numerical Integration*, Mathematical Centre Tract No. **8** (Mathematisch Centrum, Amsterdam, 1964), p. 23.